



HAL
open science

Body-fixed formulation of rotational excitation: exact and centrifugal decoupling results for CO-He

Jean-Michel Launay

► **To cite this version:**

Jean-Michel Launay. Body-fixed formulation of rotational excitation: exact and centrifugal decoupling results for CO-He. *Journal of Physics B: Atomic and Molecular Physics*, 1976, 9 (10), pp.1823 - 1838. 10.1088/0022-3700/9/10/025 . hal-01700178

HAL Id: hal-01700178

<https://hal.science/hal-01700178>

Submitted on 28 Sep 2022

HAL is a multi-disciplinary open access archive for the deposit and dissemination of scientific research documents, whether they are published or not. The documents may come from teaching and research institutions in France or abroad, or from public or private research centers.

L'archive ouverte pluridisciplinaire **HAL**, est destinée au dépôt et à la diffusion de documents scientifiques de niveau recherche, publiés ou non, émanant des établissements d'enseignement et de recherche français ou étrangers, des laboratoires publics ou privés.

Body-fixed formulation of rotational excitation: exact and centrifugal decoupling results for CO-He

To cite this article: J -M Launay 1976 *J. Phys. B: Atom. Mol. Phys.* **9** 1823

View the [article online](#) for updates and enhancements.

You may also like

- [Nonlinear suboptimal tracking control of spacecraft approaching a tumbling target](#)
Zhan-Peng Xu, , Xiao-Qian Chen et al.
- [A multibody approach for 6-DOF flight dynamics and stability analysis of the hawkmoth *Manduca sexta*](#)
Joong-Kwan Kim and Jae-Hung Han
- [Effective field theory of emergent symmetry breaking in deformed atomic nuclei](#)
T Papenbrock and H A Weidenmüller

Body-fixed formulation of rotational excitation: exact and centrifugal decoupling results for CO-He

Jean-Michel Launay

Département d'Astrophysique Fondamentale, Observatoire de Meudon, 92190 Meudon, France

Received 1 December 1975, in final form 5 February 1976

Abstract. The problem of rotational excitation of a rigid rotor is formulated in a body-fixed frame of reference. Full account is taken of the simple form of the close-coupling equations to reduce the amount of computing time.

We consider, in particular, the excitation of carbon monoxide ($^1\Sigma$ ground electronic state) by helium (1S ground electronic state) in the temperature conditions of the interstellar medium.

We also examine the validity of the centrifugal decoupling approximation. It is found that good agreement is obtained in the partial cross sections for low J , the total angular momentum, and low rotor levels; for high J , the centrifugal decoupling cross sections converge too quickly.

1. Introduction

The rotational excitation of molecules by neutral atoms (H and He) or molecules (H_2) is an important process in interstellar clouds. The knowledge of excitation cross sections is necessary to compute the populations of the molecular energy levels. In view of the low kinetic temperature of the clouds (10–100 K), quantum calculations are desirable and can now be efficiently performed for some simple systems.

The conventional formulation of the scattering of atoms in a 1S ground electronic state by linear, non-vibrating molecules in a $^1\Sigma$ ground electronic state is that of Arthurs and Dalgarno (1960); they expand the wavefunction of the total system in a space-fixed (SF) system of reference and take account of the conservation of the total angular momentum to simplify the computations. The approximation is then to take into account only a finite number of rotational levels of the molecule. However, due to the rotational degeneracy, one is faced with a fairly large number of equations to solve.

Recently, approximate methods have been proposed to reduce the complexity of the calculations: an effective potential method (Rabitz 1972) and centrifugal decoupling (CD) (McGuire and Kouri 1974, Pack 1974). The aim of both these methods is to remove the rotational degeneracy and so to decouple the molecular and relative angular momenta.

Rabitz introduced the effective potential by taking an appropriate average over the components of the diatom angular momentum; each rotational level gives rise to only one equation. McGuire and Kouri took account of the approximate conservation of Ω , the projection of the diatom angular momentum on the relative vector

(the vector joining the centres of mass). One must solve then a set of systems of coupled equations, a system for each possible value of Ω ; the maximum number of equations in each system is the number of rotor levels which are used in the expansion of the wavefunction. The CD method is best worked out in a rotating body-fixed (BF) system of reference, the relative vector being on the Oz axis. The BF formalism has been developed by Curtiss and Adler (1952), and was recently used by Pack (1974) in collision problems. The set of equations obtained using this coordinate system has the same dimensionality as the set of SF equations but its structure is different; one clearly sees the distinction between Ω couplings, due to the rotation of the relative vector, and j couplings, due to the electrostatic potential; the BF formalism takes account of the invariance of the potential for rotation about the relative vector.

This formalism was used by Neilsen and Gordon (1972) in a semiclassical treatment of the He-HCl collisions and more recently by Walker and Light (1975) in a quantum-mechanical treatment of scattering by an anisotropic Lennard-Jones potential. However the latter did not exploit the structure of the BF equations.

Here we study the rotational excitation of CO by He, taking explicitly into account the structure of the BF equations. In §2 we present the BF equations; in §3 we describe the numerical method employed, in §4 we consider the special case of CO-He scattering and in §5 we compare the CD results for this system with the exact CC results.

2. The coupled equations in the BF frame

We consider (figure 1) the scattering of atom A (1S electronic state) by the diatomic BC ($^1\Sigma$ electronic state). We shall ignore the vibrations of BC which will be considered as a rigid rotor. In all that follows, we adopt the conventions of Rose (1957) for the Euler angles and rotation matrices.

We denote the internuclear vector of molecule BC by $\mathbf{R} = \overrightarrow{BC}$ ($\hat{\mathbf{R}} = \mathbf{R}/R$) and the vector joining the centre of mass G of BC to atom A by $\mathbf{r} = \overrightarrow{GA}$ (the relative motion vector) ($\hat{\mathbf{r}} = \mathbf{r}/r$). $(Oxyz)$ is a reference frame whose axes are fixed in direction (SF frame) and $(Ox'y'z')$ is a rotating frame (BF frame). O , the centre of mass of the

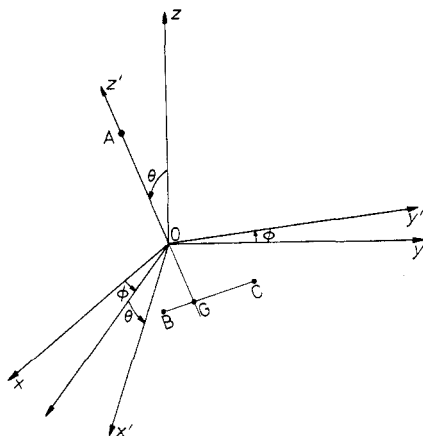


Figure 1. $(Oxyz)$ is the SF reference frame. $(Ox'y'z')$ is the BF reference frame. A rotation of Euler angles $(\phi, \theta, 0)$ brings the $(Oxyz)$ frame into the $(Ox'y'z')$ frame.

A-BC system is on GA, Oz' points in the direction of A and Oy' is chosen to lie in the xOy plane. (R, Θ, Φ) and (R, Θ', Φ') are the polar coordinates of R in the $(Oxyz)$ and $(Ox'y'z')$ frames respectively. (r, θ, ϕ) are the polar coordinates of r in the $(Oxyz)$ frame. A rotation of Euler angles $(\phi, \theta, 0)$ brings the $(Oxyz)$ frame into the $(Ox'y'z')$ frame.

The Schrödinger equation of the system A + BC after the centre of mass separation can be written (in atomic units) as

$$(H_{BC}(\hat{R}) + H_A(r) + V(r, \hat{R}) - E)\psi(r, \hat{R}) = 0 \quad (1)$$

where E is the total energy of the system. $H_{BC}(\hat{R}) = j^2/2I$ is the Hamiltonian of molecule BC, I its moment of inertia and j its angular momentum operator. $H_A(r) = p^2/2\mu$ is the Hamiltonian of atom A, $\mu = [m_A m_{BC}/(m_A + m_{BC})]$ is the reduced mass of the A-BC system where m_A is the mass of A and m_{BC} the mass of BC.

Due to the invariance of the potential under rotations of the system and under inversions in the origin, it is convenient to write the wavefunction as a sum of different components of definite total angular momentum $J = j + l$ (where l is the relative angular momentum) and definite total parity ϵ (ϵ denotes the eigenvalues of Π , the inversion operator in the origin 0). More precisely J^2 , J_z and Π commute with H and so J , M and ϵ are conserved during the collision.

$$\psi(r, \hat{R}) = \sum_{JM\epsilon} c_{JM\epsilon} \psi^{JM\epsilon}(r, \hat{R}).$$

The coefficients $c_{JM\epsilon}$ are chosen such that $\psi(r, \hat{R})$ satisfies the usual boundary conditions (Arthurs and Dalgarno 1960). Then the $\psi^{JM\epsilon}(r, \hat{R})$ can be expanded over a complete set of eigenfunctions of J^2 , J_z , Π , j^2 , l^2 formed by vector coupling of spherical harmonics:

$$Y_{jl}^{JM\epsilon}(\hat{r}, \hat{R}) = \sum_{m_j m_l} (-)^{j-l+M} (2J+1)^{1/2} \begin{pmatrix} j & l & J \\ m_j & m_l & -M \end{pmatrix} Y_{jm_j}(\Theta, \Phi) Y_{lm_l}(\theta, \phi) \quad (2)$$

where

$$\begin{pmatrix} a & b & c \\ \alpha & \beta & \gamma \end{pmatrix}$$

denotes a $3j$ symbol. The parity $\epsilon = (-)^{j+l}$.

We thus obtain the expansion employed by Arthurs and Dalgarno (1960) which can be written as

$$\psi^{JM\epsilon}(r, \hat{R}) = \sum_{jl} \frac{1}{r} G_{jl}^{J\epsilon}(r) Y_{jl}^{JM\epsilon}(\hat{r}, \hat{R}) \quad (3)$$

where the sum is over (j, l) values such that $(-)^{j+l} = \epsilon$. Another possibility is to expand the $\psi^{JM\epsilon}(r, \hat{R})$ over a complete set of eigenfunctions of J^2 , J_z , j^2 , $|j_z|$, Π . This was done by Curtiss and Adler (1952) and more recently by Pack (1974).

We first consider eigenfunctions of J^2 , J_z , j^2 , j_z :

$$Y_{j\Omega}^{JM}(\hat{r}, \hat{R}) = N_{M\Omega}^J(\theta, \phi) Y_{j\Omega}(\Theta', \Phi') \quad (4)$$

where $N_{M\Omega}^J(\theta, \phi) = [(2J+1)/4\pi]^{1/2} D_{M\Omega}^{J*}(\phi, \theta, 0)$ are normalized symmetric top wavefunctions and \mathbf{D} is a rotation matrix (Rose 1957).

To get eigenfunctions of definite total parity, we must take a linear combination

of the $+\Omega$ and $-\Omega$ components; these functions will no longer be eigenfunctions of j_z , but of $|j_z|$. Denoting $\bar{\Omega} = |\Omega|$ we get (see appendix 1)

$$Y_{j\bar{\Omega}}^{JM\epsilon}(\hat{r}, \hat{R}) = (Y_{j\bar{\Omega}}^{JM}(\hat{r}, \hat{R}) + \epsilon(-)^J Y_{j-\bar{\Omega}}^{JM}(\hat{r}, \hat{R}))/2^{1/2}(1 + \delta_{\bar{\Omega}0})^{1/2} \tag{5}$$

where $\bar{\Omega} = 0, 1, \dots, \min(j, J)$ if $\epsilon = (-)^J$ and $\bar{\Omega} = 1, \dots, \min(j, J)$ if $\epsilon = (-)^{J+1}$. In appendix 2, we show that between the two sets of eigenfunctions (2) and (5), we have the unitary transformation \mathbf{P} :

$$Y_{j\bar{\Omega}}^{JM\epsilon}(\hat{r}, \hat{R}) = \sum_{\bar{\Omega}} P_{\bar{\Omega}}^{JM\epsilon;j} Y_{j\bar{\Omega}}^{JM\epsilon}(\hat{r}, \hat{R}) \tag{6}$$

where

$$P_{\bar{\Omega}}^{JM\epsilon;j} = (-)^{J+\bar{\Omega}} 2^{1/2} (2l + 1)^{1/2} \begin{pmatrix} j & J & l \\ \bar{\Omega} & -\bar{\Omega} & 0 \end{pmatrix} (1 + \delta_{\bar{\Omega}0})^{-1/2}.$$

The corresponding expansion of the wavefunction is

$$\psi^{JM\epsilon}(r, \hat{R}) = - \sum_{j\bar{\Omega}} \frac{1}{r} G_{j\bar{\Omega}}^{J\epsilon}(r) Y_{j\bar{\Omega}}^{JM\epsilon}(\hat{r}, \hat{R}). \tag{7}$$

The Schrödinger equation (1) can be written, using

$$p^2 = \frac{1}{r} \frac{\partial^2}{\partial r^2} r + \frac{l^2}{r^2}$$

and the expansion (7), as

$$\frac{d^2}{dr^2} G_{j\bar{\Omega}}^{J\epsilon}(r) + \sum_{j'\bar{\Omega}'} W_{j\bar{\Omega},j'\bar{\Omega}'}^{J\epsilon}(r) G_{j'\bar{\Omega}'}^{J\epsilon}(r) = 0 \tag{8}$$

where

$$W_{j\bar{\Omega},j'\bar{\Omega}'}^{J\epsilon} = \delta_{jj'} \delta_{\bar{\Omega}\bar{\Omega}'} k_j^2 - \frac{1}{r^2} \langle Y_{j\bar{\Omega}}^{JM\epsilon} | l^2 | Y_{j'\bar{\Omega}'}^{JM\epsilon} \rangle - 2\mu \langle Y_{j\bar{\Omega}}^{JM\epsilon} | V | Y_{j'\bar{\Omega}'}^{JM\epsilon} \rangle.$$

The wavenumber in channel $j\bar{\Omega}$ is defined by $k_j^2 = 2\mu[E - j(j + 1)/2I]$.

l^2 couples channels $j\bar{\Omega}$ and $j'\bar{\Omega}'$ with $j' = j$, $\bar{\Omega}' = \bar{\Omega} - 1$, $\bar{\Omega}$, $\bar{\Omega} + 1$. All matrix elements are obtained using (see appendix 3)

$$\langle Y_{j\bar{\Omega}}^{JM\epsilon} | l^2 | Y_{j\bar{\Omega}}^{JM\epsilon} \rangle = J(J + 1) + j(j + 1) - 2\bar{\Omega}^2 \tag{9}$$

$$\langle Y_{j\bar{\Omega}}^{JM\epsilon} | l^2 | Y_{j\bar{\Omega}\pm 1}^{JM\epsilon} \rangle = -(1 + \delta_{\bar{\Omega}0})^{1/2} \{ [J(J + 1) - \bar{\Omega}(\bar{\Omega} \pm 1)] [j(j + 1) - \bar{\Omega}(\bar{\Omega} \pm 1)] \}^{1/2}.$$

The potential $V(r, \hat{R})$ is expanded in Legendre polynomials:

$$V(r, \hat{R}) = \sum_{\lambda=0}^{\lambda_{\max}} v_{\lambda}(r) P_{\lambda}(\hat{r}, \hat{R}). \tag{10}$$

Using (10), we obtain

$$\begin{aligned} \langle Y_{j\bar{\Omega}}^{JM\epsilon} | V | Y_{j'\bar{\Omega}'}^{JM\epsilon} \rangle \\ = \delta_{\bar{\Omega}\bar{\Omega}'} \sum_{\lambda=0}^{\lambda_{\max}} (-)^{\bar{\Omega}} [(2j + 1)(2j' + 1)]^{1/2} \begin{pmatrix} j & j' & \lambda \\ 0 & 0 & 0 \end{pmatrix} \begin{pmatrix} j & j' & \lambda \\ \bar{\Omega} - \bar{\Omega} & 0 & 0 \end{pmatrix} v_{\lambda}(r). \end{aligned} \tag{11}$$

Only couples channels $j\bar{\Omega}$ with channels $j'\bar{\Omega}$ because the potential depends only on the angle between \hat{r} and \hat{R} .

Using relations (3), (7), and the unitary transformation (6) we can derive the following relations:

$$G_{j\Omega}^{J\epsilon}(r) = \sum_{\bar{\Omega}} P_{i\bar{\Omega}}^{JM\epsilon:j} G_{j\bar{\Omega}}^{J\epsilon}(r) \quad (12)$$

$$G_{j\bar{\Omega}}^{J\epsilon}(r) = \sum_l P_{i\bar{\Omega}}^{JM\epsilon:j} G_{jl}^{J\epsilon}(r). \quad (13)$$

Relation (12) is useful to go from the BF to the SF representation.

One may summarize the form of the BF coupled equations by a sketch of the coupling matrix $\mathbf{W}^{J\epsilon}(r)$ (see figure 2). The matrix $\mathbf{W}^{J\epsilon}(r)$ has a large number of zero elements: for example, with the basis 0-7, out of the $36 \times 36 = 1296$ total number of elements (parity $\epsilon = (-)^J$), only 260 are non-zero.

3. Numerical integration of the BF equations

The special form of the $\mathbf{W}^{J\epsilon}(r)$ matrix suggests that it is advantageous to integrate the BF equations rather than the SF equations.

We used the De Vogelaere (1955) algorithm which was found by Allison (1970) to be faster than the usual Numerov method (see also Lester 1971). In addition, it enables full advantage to be taken of the form of the $\mathbf{W}^{J\epsilon}(r)$ matrix. For completeness we briefly state the algorithm in matrix form.

Given the system of equations

$$\left(\mathbf{I} \frac{d^2}{dr^2} + \mathbf{W}^{J\epsilon}(r) \right) \mathbf{G}^{J\epsilon}(r) = 0$$

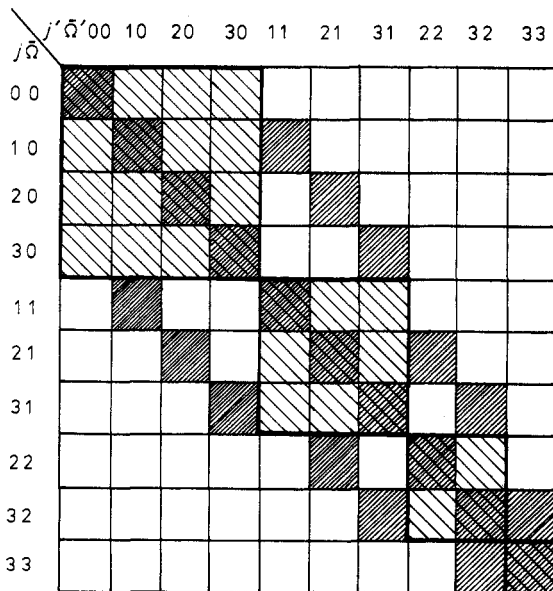


Figure 2. A sketch of the $\mathbf{W}^{J\epsilon}(r)$ coupling matrix. Basis $j = 0-3$, parity $\epsilon = (-)^J$. I^2 matrix elements are found in the dark hatched squares. V matrix elements are found in the light hatched squares. The case $\epsilon = (-)^{J+1}$ may be found by striking out rows and columns with $\bar{\Omega} = 0, \bar{\Omega}' = 0$. The case $J < 3$ may be found by striking out rows and columns with $\bar{\Omega} > J, \bar{\Omega}' > J$.

where N is the number of channels, \mathbf{I} is the $N \times N$ identity square matrix and $\mathbf{G}^{J\epsilon}(r)$ is the $N \times N$ matrix of solution vectors (each column represents a solution vector). Integration from r_n to r_{n+1} is performed using an intermediate point $r_{n+1/2} = \frac{1}{2}(r_n + r_{n+1})$. Putting $h = r_{n+1} - r_n$, we perform the following operations:

$$\begin{aligned} \mathbf{G}_{n+1/2}^{J\epsilon} &= \mathbf{G}_n^{J\epsilon} + \frac{1}{2}h\mathbf{G}_n^{J\epsilon} - \frac{1}{24}h^2(4\mathbf{W}_n^{J\epsilon}\mathbf{G}_n^{J\epsilon} - \mathbf{W}_{n-1/2}^{J\epsilon}\mathbf{G}_{n-1/2}^{J\epsilon}) \\ \mathbf{G}_{n+1}^{J\epsilon} &= \mathbf{G}_n^{J\epsilon} + h\mathbf{G}_n^{J\epsilon} - \frac{1}{6}h^2(\mathbf{W}_n^{J\epsilon}\mathbf{G}_n^{J\epsilon} + 2\mathbf{W}_{n+1/2}^{J\epsilon}\mathbf{G}_{n+1/2}^{J\epsilon}) \\ \mathbf{G}_{n+1}^{J\epsilon} &= \mathbf{G}_n^{J\epsilon} - \frac{1}{6}h(\mathbf{W}_n^{J\epsilon}\mathbf{G}_n^{J\epsilon} + 4\mathbf{W}_{n+1/2}^{J\epsilon}\mathbf{G}_{n+1/2}^{J\epsilon} + \mathbf{W}_{n+1}^{J\epsilon}\mathbf{G}_{n+1}^{J\epsilon}) \end{aligned} \quad (14)$$

where $\mathbf{X}_p = \mathbf{X}(r_p)$ and where \mathbf{X} represents \mathbf{W} or \mathbf{G} ; $\mathbf{G}' = d\mathbf{G}/dr$. Integration is started from r_0 , chosen sufficiently far in the classically forbidden region, using

$$\mathbf{G}_0^{J\epsilon} = 0 \quad \text{and} \quad \mathbf{G}_{-1/2}^{J\epsilon} = -\frac{1}{2}h\mathbf{G}_0^{J\epsilon}.$$

$\mathbf{G}_0^{J\epsilon}$ is an arbitrary nonsingular matrix. The time-consuming operations when propagating the matrix $\mathbf{G}_n^{J\epsilon}$ to $\mathbf{G}_{n+1}^{J\epsilon}$ are the two matrix multiplications $\mathbf{W}_{n+1/2}^{J\epsilon}\mathbf{G}_{n+1/2}^{J\epsilon}$ and $\mathbf{W}_{n+1}^{J\epsilon}\mathbf{G}_{n+1}^{J\epsilon}$ in the algorithm (14).

If $\mathbf{W}_p^{J\epsilon}$ is a full matrix, as in the SF case, N^3 additions and multiplications are needed for each matrix multiplication. The other operations in the algorithm (matrix additions and matrix multiplication by a scalar) require only about N^2 elementary operations and thus are rapidly performed. However, $\mathbf{W}_p^{J\epsilon}$ in the BF case has only $N_0 \ll N^2$ non-zero elements. The multiplication of each column vector of \mathbf{G}_p by \mathbf{W}_p requires N_0 additions and multiplications (it should be remembered that \mathbf{G}_p is a full matrix). Hence each matrix multiplication requires $N_0 \times N \ll N^3$ additions and multiplications. The advantage in speed is a factor of $1296/260 \sim 5$ for the 36-channel calculation we considered above. More generally, for rotational excitation, we have $N_0 \sim N^{1.5}$, thus the computational time should increase as $N^{2.5}$ in the BF representation instead of as N^3 in the SF representation. The same relative advantage in computing time could be achieved using different numerical methods. The advantage is very easily obtained when the method involves only matrix multiplications as in the De Vogelaere, Stormer (Choi and Tang 1975) or Sams-Kouri (1969) algorithms; when matrix diagonalizations as in the Gordon (1971) and Light (1971) algorithms are needed, somewhat more programming is necessary.

3.1. Boundary conditions

The coupled equations must be integrated in a range $r \in [r_0, r_f]$ where r_f is sufficiently large such that the radial functions have reached their asymptotic form. However, due to the non-diagonal elements of I^2 , the asymptotic form of the BF solutions is more complicated than the asymptotic form of the SF solutions. Of course, it would be possible to integrate the equations to a point r_f' where, to good accuracy, the centrifugal coupling terms can be put to zero; however they decay as r^{-2} , much slower than the potential terms which for neutral systems decay as r^{-6} , so this procedure would yield $r_f' \gg r_f$ and would be wasteful of computing time.

To get the \mathbf{S} matrix and cross sections, starting from the BF solutions at r_f , we have two possibilities.

(i) We can get an analytical form of the asymptotic solutions and then fit the integrated BF solution to these asymptotic solutions. This procedure yields a BF \mathbf{S} matrix.

(ii) By means of relation (12), we can convert the BF solutions to SF at r_f . We get SF solutions and derivatives:

$$\begin{aligned} \mathbf{G}_{\text{SF}}^{J\epsilon}(r_f) &= \mathbf{P}^{J\epsilon} \mathbf{G}_{\text{BF}}^{J\epsilon}(r_f) \\ \mathbf{G}'_{\text{SF}}^{J\epsilon}(r_f) &= \mathbf{P}^{J\epsilon} \mathbf{G}'_{\text{BF}}^{J\epsilon}(r_f). \end{aligned}$$

These are then fitted to standard Bessel functions to yield a SF $\mathbf{K}^{J\epsilon}$ matrix (see for example Gordon 1971).

From the $\mathbf{K}^{J\epsilon}$ matrix, we get $\mathbf{T}^{J\epsilon} = -2i\mathbf{K}^{J\epsilon}(\mathbf{I} - i\mathbf{K}^{J\epsilon})^{-1}$. Partial cross sections are obtained from the usual formulae (Arthurs and Dalgarno 1960).

$$\sigma^J(j_0, j) = \frac{\pi}{k_{j_0}^2} \frac{(2J+1)}{(2j_0+1)} \sum_{\epsilon l l_0} |T_{jl; j_0 l_0}^{J\epsilon}|^2$$

and total cross sections are given by

$$\sigma(j_0, j) = \sum_J \sigma^J(j_0, j)$$

where $\sigma(j_0, j)$ denotes the cross section for transitions from j_0 to j .

3.2. Centrifugal decoupling

This approximation of the BF equations was introduced by McGuire and Kouri (1974) in a close-coupling study and by Pack (1974) using the sudden approximation. If, in the SF equations, we put $\langle Y_{jl}^{JM\epsilon} | l^2 | Y_{j'l'}^{JM\epsilon} \rangle = J(J+1)\delta_{jj'}\delta_{ll'}$ instead of $l(l+1)\delta_{jj'}\delta_{ll'}$ which is the exact value, we get, using the unitary transformation $\mathbf{P}^{J\epsilon}$ of the BF equations,

$$\langle Y_{j\bar{\Omega}}^{JM\epsilon} | l^2 | Y_{j'\bar{\Omega}}^{JM\epsilon} \rangle = J(J+1)\delta_{jj'}\delta_{\bar{\Omega}\bar{\Omega}}. \quad (15)$$

The BF equations separate into smaller subsystems, each subsystem corresponding to a possible value of $\bar{\Omega}$ which is then a good quantum number. Boundary conditions may now be imposed in the BF frame at about the same point r_f , since the off-diagonal l^2 matrix elements are zero (see McGuire and Kouri 1974). Furthermore, we note that the BF equations no longer depend on ϵ . Hence $T_{j\bar{\Omega}; j_0 \bar{\Omega}_0}^{J\epsilon} = \delta_{\bar{\Omega}\bar{\Omega}_0} T_{j\bar{\Omega}; j_0 \bar{\Omega}_0}^J$ except when $\epsilon = (-)^{j+1}$ and j or $j_0 = 0$ when the matrix element is 0.

Partial cross sections are obtained using the formulae

$$\begin{aligned} \sigma^J(j_0, j) &= \frac{\pi}{k_{j_0}^2} \frac{(2J+1)}{(2j_0+1)} 2 \sum_{\bar{\Omega}} |T_{j\bar{\Omega}; j_0 \bar{\Omega}}^J|^2 & \text{if } j_0, j \neq 0 \\ \sigma^J(j_0, j) &= \frac{\pi}{k_{j_0}^2} \frac{(2J+1)}{(2j_0+1)} |T_{j_0; j_0 0}^J|^2 & \text{if } j_0 \text{ or } j = 0. \end{aligned}$$

We can also use the exact value of the diagonal l^2 matrix element:

$$\langle Y_{j\bar{\Omega}}^{JM\epsilon} | l^2 | Y_{j\bar{\Omega}}^{JM\epsilon} \rangle = \delta_{jj} \delta_{\bar{\Omega}\bar{\Omega}} [J(J+1) + j(j+1) - 2\bar{\Omega}^2]. \quad (16)$$

We shall refer to the approximation in (15) as CD1 and to the approximation in (16) as CD2. The form of CD2 requires spherical Bessel functions of order λ such that $\lambda(\lambda+1) = J(J+1) + j(j+1) - 2\bar{\Omega}^2$. λ is, in general, a real number. Spherical Bessel functions may conveniently be calculated in terms of cylindrical Bessel functions (Abramowitz and Stegun 1965).

Table 1. The numerical potential derived from the electron-gas model calculated by Green and Thaddeus (1976). Distances are in au; the potential is given in cm^{-1} . For distances greater than 10 au, v_0 , v_1 , v_2 are computed using the asymptotic expansions given by Green and Thaddeus (1976).

r	v_0	v_1	v_2	v_3	v_4	v_5
2.0	147877.44	-26995.36	237906.88	-73432.69	112346.69	-38811.91
2.5	56292.16	-6107.16	77524.44	-17033.82	25603.37	-6854.55
3.0	22810.08	-5500.67	32135.48	-7508.60	9277.00	-2184.46
3.5	9028.87	-4088.17	13896.86	-4083.16	4015.20	-1046.75
4.0	3342.32	-2363.14	5795.38	-2104.56	1757.68	-506.61
4.5	1110.34	-1136.28	2268.45	-980.59	737.95	-231.81
5.0	298.91	-467.96	812.18	-415.89	295.38	-100.49
5.5	37.59	-159.01	251.29	-159.53	111.81	-41.43
6.0	-18.71	-35.49	54.47	-53.09	39.20	-16.33
6.5	-21.87	3.41	-2.95	-13.12	12.19	-6.01
7.0	-16.60	8.94	-10.47	-0.16	2.86	-1.90
7.5	-13.00	7.68	-8.89	1.88	0.02	-0.31
8.0	-10.20	5.08	-5.73	1.75	-0.65	0.26
8.5	-7.90	2.96	-3.26	1.13	-0.59	0.43
9.0	-5.92	1.63	-1.73	0.59	-0.34	0.31
9.5	-4.28	0.88	-0.86	0.28	-0.18	0.21
10.0	-3.14	0.49	-0.53	0.12	0.0	0.0

4. Application to CO-He scattering

4.1. Potential surface

We employed a potential surface calculated by Green and Thaddeus (1976) using the Gordon-Kim uniform electron-gas model (1972) at short and intermediate distances (near the Van der Waals minimum) and perturbation theory at large distances to take properly into account the dispersion and induction forces. The Legendre expansion of the potential is given in table 1. For the rotational constant, we used $B_{\text{CO}} = 1.92265 \text{ cm}^{-1}$ †.

4.2. Collision dynamics

Calculations were performed in the CC and CD1-2 methods including all open channels in the expansion of the wavefunctions. The error introduced by this approximation is thought not to be very large. Tests were made which indicated that the CC and CD methods had similar rates of convergence. The same conclusion was reached by McGuire (1976) for the He-HCN system and Green (1976) for the He-CO system.

At an energy of 130 cm^{-1} where the basis $j = 0-7$ was used, two sets of 36 and 28 equations are solved corresponding to the two parities at each J value in the CC method while in the CD methods, we have 8 systems of 8, 7, ..., 1 equations at each J value. At this energy, we sum up to $J = 35$ to get converged inelastic as well as elastic total cross sections. The total computing time was 310 s for CC and 39 s for CD on an IBM 370/168 computer. The conventional SF-CC calculation would take about 1000 s. Storage requirements are 170 kbytes for CC and 90 kbytes for CD. The computations were made using integration limits and step sizes such that the numerical uncertainty in the cross sections would not exceed 2%; \mathbf{K} -matrix symmetry was in general better than three significant figures.

† $1 \text{ cm}^{-1} = 1.4388 \text{ K} = 1.2399 \times 10^{-4} \text{ eV}$.

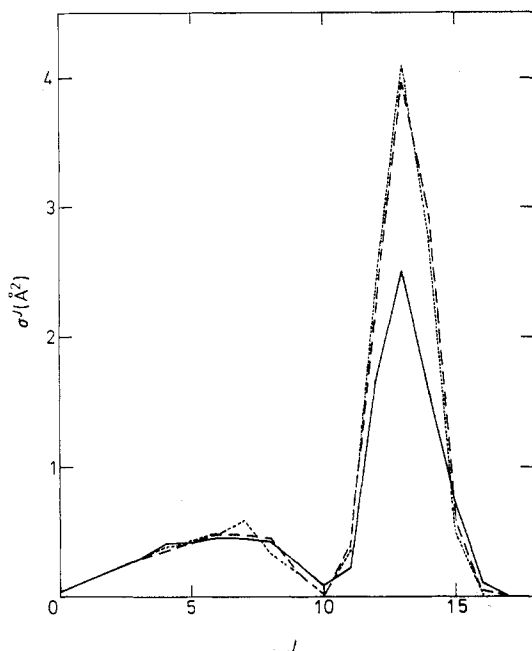


Figure 3. $\sigma^J(0, 1)$ at an energy of 50 cm^{-1} . Full curve, CC results; broken curve, CD1 results; dotted curve, CD2 results.

5. Results and discussion

5.1. Inelastic cross sections

He-CO is a system whose short-range anisotropy is large whereas the long-range anisotropy is rather small. Hence, inelastic collisions will sample mainly the repulsive part of the potential at higher energies and the potential well at lower energies. The long-range Van der Waals forces are rather ineffective except at very low energies. In figures 3 and 4 we have plotted $\sigma^J(0, 1)$ and $\sigma^J(0, 2)$ at an energy of 50 cm^{-1} . Short-

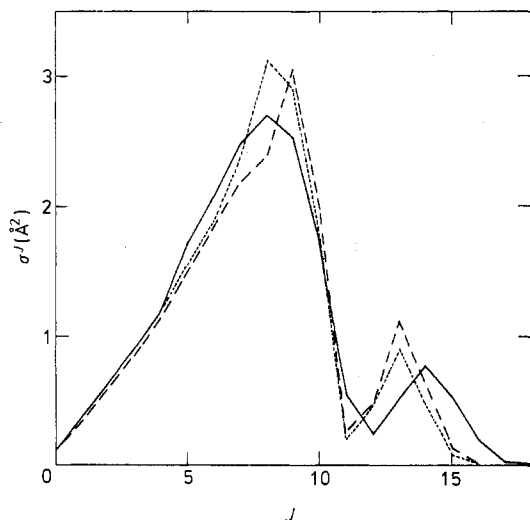


Figure 4. $\sigma^J(0, 2)$ at an energy of 50 cm^{-1} . CC, CD1 and CD2 results as in figure 3.

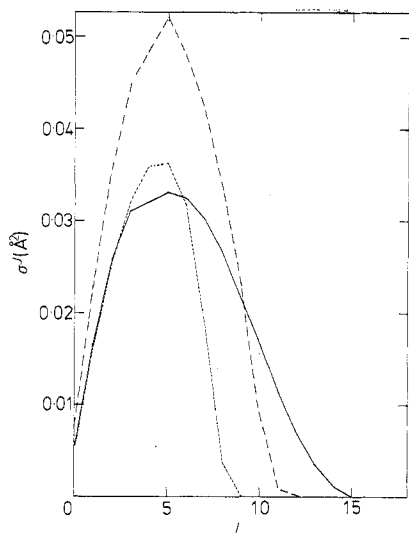


Figure 5. $\sigma^J(0, 7)$ at an energy of 130cm^{-1} . CC, CD1 and CD2 results as in figure 3.

range forces are dominant for low partial waves and long-range forces for high partial waves. CD1 and CD2 are in good agreement with CC for low J whereas for high J we see discrepancies in $\sigma^J(0, 1)$. We note that for these cross sections CD1 and CD2 are in close agreement but converge too quickly with J for the 0-2 transition.

In figure 5 we plot $\sigma^J(0, 7)$ at an energy of 130cm^{-1} . CD2 agrees closely with CC at very low J but converges much too quickly. CD1 is higher at low J and also converges too quickly with J .

The behaviour of the cross sections may be explained as follows: in collisions where a high angular momentum is transferred to the molecule, the angular momentum of the incident particle is decreased and hence scattering occurs mainly from channels $j = 0, l = J$ to j', l' with $l' < J$; but for these channels the CD1 treatment puts up too large a repulsive barrier, since it assumes $l' = J$. Hence the probability of excitation in these channels is decreased and, since they are the most important, the total

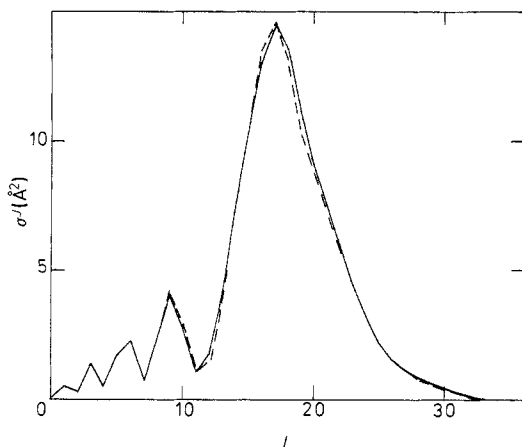


Figure 6. $\sigma^J(0, 0)$ at an energy of 130cm^{-1} . Full curve, CC results; broken curve, CD1 and CD2 results (indistinguishable to graphical accuracy).

excitation probability is decreased. For small J on the contrary, scattering occurs mainly from $j = 0, l = J$ to j', l' with $l' > J$ (this is obvious for $J = 0$ since then the only possibility is $l' = j'$) and putting $l' = J$ lowers the centrifugal barrier; excitation cross sections are enhanced in CD1. Now CD2 is an exact treatment of the BF equations for $J = 0$ since, for this value, we have no off-diagonal centrifugal coupling terms (it was verified numerically that CD2 and CC gave the same results for $J = 0$); thus it is not surprising that CD2 and CC are in good agreement for low J . For higher J , CD2 should in general be smaller than CD1, since in the BF formulation scattering occurs from $j = 0, \bar{\Omega} = 0$ to $j', \bar{\Omega}' = 0$, the centrifugal barrier being $J(J + 1)/r^2$ in CD1 and $[(J(J + 1) + j'(j' + 1))/r^2]$ in CD2.

5.2. Elastic cross sections

Elastic collisions are less sensitive to CD approximations since they sample mainly the isotropic part of the potential, and for an isotropic potential and $j = 0$, CD1 and CD2 are identical with CC. Consider, for example, figure 6 where we have plotted $\sigma^J(0, 0)$ at $E = 130 \text{ cm}^{-1}$. CC, CD1, CD2 practically agree to graphical accuracy. In figures 7 and 8 we have plotted $\sigma^J(2, 2)$ and $\sigma^J(5, 5)$ at $E = 130 \text{ cm}^{-1}$. For $\sigma^J(2, 2)$, we see that CC smoothes out the low J oscillations of CD; CD1 and CD2 are in close agreement. For $\sigma^J(5, 5)$, discrepancies are clearly seen; the maxima in CD are much higher than in CC but the partial cross sections converge too quickly; CD2 does not appear to be better than CD1. This behaviour in $\sigma^J(j, j)$ may reflect the fact that CC results are a mean of CD1 results over the range $|J - j|$ to $J + j$ (in CC, l can vary from $|J - j|$ to $J + j$ and in CD1 we have $l = J$). In table 2, we give the total cross sections between different rotational levels at 50 cm^{-1} . One can see that CD gives very good results for the 0–2 transition which, as we have seen before, is mainly due to short-range forces. In general, CD2 underestimates cross sections between excited rotor-levels.

5.3. Interaction potential

To see the influence of the potential on the cross sections, we decided to make an exponential fit to the potential. Each member of the Legendre expansion can, to good

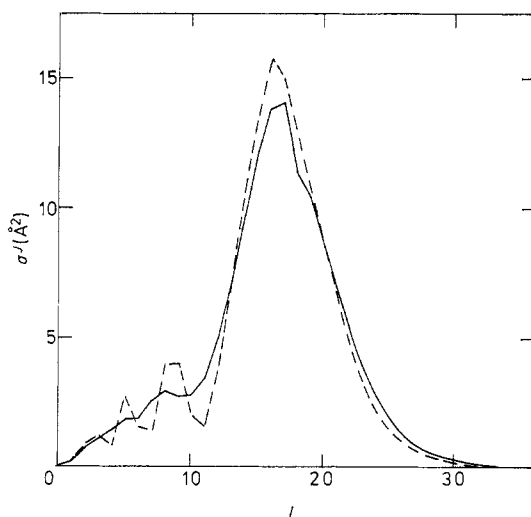


Figure 7. $\sigma^J(2, 2)$ at an energy of 130 cm^{-1} . CC, CD1 and CD2 results as in figure 6.

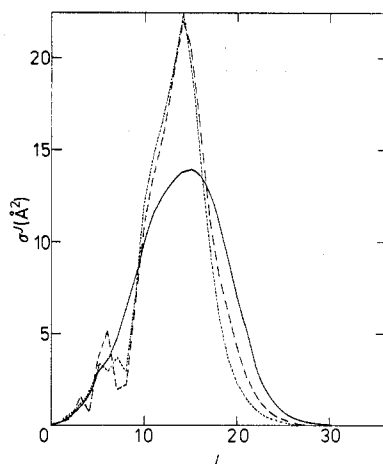


Figure 8. $\sigma^j(5, 5)$ at an energy of 130 cm^{-1} . CC, CD1 and CD2 results as in figure 3.

accuracy, be fitted to an exponential in the region $r < 4.5\text{ au}$. We then take $v_i^{\text{exp}}(r) = a_i \exp(-\alpha r)$ for all r , with $\alpha = 1.85\text{ au}^{-1}$. The a_i are determined such that the two potentials coincide exactly at 4 au . This potential is clearly of short range. We can see in table 3 that the CD1 results are now in much better agreement with CC. We note that McGuire and Kouri (1974) obtained similar agreement for He-H₂ collisions (although at much higher energies), where the potential employed also decayed exponentially with r . Finally, we should point out that the cross sections changed by roughly an order of magnitude except for $\Delta j = 2$ transitions; this illustrates the importance of the Van der Waals minimum in determining the cross sections.

6. Conclusion

We have shown that, using the De Vogelaere integration method, we can take account of the symmetry of the BF equations to reduce the amount of computation by a factor

Table 2. Total cross sections at an energy of 50 cm^{-1} using CC, CD1 and CD2 methods with the electron-gas model potential; cross sections are in \AA^2 .

Cross sections	CC	CD1	CD2
0-0	180	176	178
0-1	9.97	13.2	13.3
0-2	19.1	18.5	18.9
0-3	3.14	2.31	2.34
0-4	3.26	3.90	2.94
1-1	193	190	191
1-2	7.72	8.06	7.56
1-3	12.0	12.0	11.8
1-4	2.40	2.38	2.36
2-2	194	189	191
2-3	7.56	6.11	5.14
2-4	9.40	10.9	8.95
3-3	203	201	199
3-4	6.56	4.65	4.63
4-4	169	145	123

Table 3. Total cross sections at an energy of 50cm^{-1} using CC and CD1 methods with the exponential fit of the electron-gas model potential; cross sections are in \AA^2 .

Cross section	CC	CD1
0-0	75.5	74.6
0-1	1.73	1.72
0-2	12.8	13.2
0-3	0.601	0.618
0-4	0.371	0.391
1-1	84.2	83.8
1-2	1.52	1.54
1-3	5.23	5.25
1-4	0.163	0.170
2-2	86.4	84.6
2-3	1.07	1.08
2-4	1.46	1.32
3-3	90.8	85.6
3-4	0.781	0.731
4-4	98.7	80.2

of about three. This method allows us to calculate very efficiently rotational excitation cross sections for many systems of astrophysical interest.

We have also used centrifugal decoupling methods which are obtained by neglecting the Coriolis coupling terms in the BF equations. These methods are found to converge too quickly with J for partial cross sections involving excited rotor levels. When using a short-range exponential potential, very good results are obtained. For the He-CO system, which shows a rather small long-range anisotropy, we get sufficiently accurate results for the total cross sections.

Acknowledgments

I would like to thank D Flower and H Van Regemorter for their continuing interest in this work and N Tran Minh for a critical reading of the manuscript; I would also like to thank P McGuire for a number of useful discussions.

Appendix 1. Parity

We calculate

$$\Pi Y_{j\Omega}^{JM}(\hat{r}, \hat{R}) = Y_{j\Omega}^{JM}(-\hat{r}, -\hat{R}).$$

The polar coordinates of $-\hat{r}$ are $(\pi - \theta, \phi + \pi)$ and the BF polar coordinates of $-\hat{R}$ are $(\Theta', \pi - \Phi')$. Then, using the relations

$$D_{M\Omega}^J(\phi + \pi, \pi - \theta, 0) = (-)^J D_{M-\Omega}^J(\phi, \theta, 0)$$

and

$$Y_{j\Omega}(\Theta', \pi - \Phi') = Y_{j-\Omega}(\Theta', \Phi')$$

we get

$$\Pi Y_{j\Omega}^{JM}(\hat{r}, \hat{R}) = (-)^J Y_{j-\Omega}^{JM}(\hat{r}, \hat{R}).$$

The functions

$$Y_{j\Omega}^{JM}(\hat{r}, \hat{R}) + \epsilon \Pi Y_{j\Omega}^{JM}(\hat{r}, \hat{R})$$

where $\epsilon = \pm 1$ have parity ϵ and norm $[2(1 + \delta_{\bar{\Omega}0})]^{1/2}$. Thus we have

$$Y_{j\Omega}^{JM\epsilon}(\hat{r}, \hat{R}) = [Y_{j\Omega}^{JM}(\hat{r}, \hat{R}) + \epsilon(-)^J Y_{j-\bar{\Omega}}^{JM}(\hat{r}, \hat{R})]/[2(1 + \delta_{\bar{\Omega}0})]^{1/2}.$$

Appendix 2. Unitary transformation

We calculate first

$$\langle j\Omega JM | j l JM \epsilon \rangle = \int Y_{j\Omega}^{JM*}(\hat{r}, \hat{R}) Y_{jl}^{JM\epsilon}(\hat{r}, \hat{R}) d\hat{r} d\hat{R}.$$

Using equations (2) and (4) and the rotation theorem of spherical harmonics,

$$Y_{j\Omega}(\Theta', \Phi') = \sum_{\Omega'} D_{\Omega'\Omega}^j(\phi, \theta, 0) Y_{j\Omega}(\Theta, \Phi)$$

we get

$$\begin{aligned} \langle j\Omega JM | j l JM \epsilon \rangle &= \left(\frac{2J+1}{4\pi}\right)^{1/2} \sum_{m_j, m_l} (-)^{j-l+M} (2J+1)^{1/2} \begin{pmatrix} j & l & J \\ m_j & m_l & -M \end{pmatrix} \\ &\times \int Y_{j\Omega}^*(\hat{R}) Y_{m_j}(\hat{R}) d\hat{R} \int D_{\Omega'\Omega}^{j*}(\hat{r}) Y_{l m_l}(\hat{r}) D_{M\Omega}^J(\hat{r}) d\hat{r} \end{aligned} \tag{A.1}$$

where

$$D_{mm}^k(\hat{r}) \equiv D_{mm}^k(\phi, \theta, 0).$$

Then, using

$$Y_{l m_l}(\hat{r}) = \left(\frac{2l+1}{4\pi}\right)^{1/2} D_{m_l 0}^{l*}(\hat{r}),$$

the second integral reduces to

$$\int D_{\Omega'\Omega}^{j*}(\hat{r}) Y_{l m_l}(\hat{r}) D_{M\Omega}^J(\hat{r}) d\hat{r} = (-)^{M+\Omega} [4\pi(2l+1)]^{1/2} \begin{pmatrix} j & l & J \\ \Omega' & m_l & -M \end{pmatrix} \begin{pmatrix} j & l & J \\ \Omega & 0 & -\Omega \end{pmatrix}. \tag{A.2}$$

Using (A.1) and (A.2) we get

$$\begin{aligned} \langle j\Omega JM | j l JM \epsilon \rangle &= (-)^{j-l+\Omega} (2l+1)^{1/2} \begin{pmatrix} j & l & J \\ \Omega & 0 & -\Omega \end{pmatrix} (2J+1) \sum_{m_j, m_l} \begin{pmatrix} j & l & J \\ m_j & m_l & -M \end{pmatrix}^2 \\ &= (-)^{j+\Omega} (2l+1)^{1/2} \begin{pmatrix} j & J & l \\ \Omega & -\Omega & 0 \end{pmatrix}. \end{aligned}$$

Using relation (5), we get

$$\langle j\bar{\Omega} JM \epsilon' | j l JM \epsilon \rangle = (-)^{j+\bar{\Omega}} (2l+1)^{1/2} \begin{pmatrix} j & J & l \\ \bar{\Omega} & -\bar{\Omega} & 0 \end{pmatrix} (1 + \epsilon\epsilon')/2^{1/2} (1 + \delta_{\bar{\Omega}0})^{1/2}$$

from which (6) may be obtained if we put $\epsilon' = \epsilon$.

Appendix 3. Matrix elements

A3.1. l^2 matrix elements

We shall first evaluate l^2 matrix elements in the $|j\Omega JM\rangle$ basis; we have

$$l^2 = (J - j)^2 = J^2 + j^2 - 2j_z^2 - (j'_+ J'_- + j'_- J'_+)$$

where we have used the relation $j_{z'} = J_{z'}$ and where the prime index denotes the components of the operators on the BF axes. Using relation (4) and the usual relations

$$j'_\pm Y_{j\Omega} = \alpha_\pm(j, \Omega) Y_{j\Omega \pm 1}$$

where

$$\alpha_\pm(a, b) = [a(a + 1) - b(b \pm 1)]^{1/2}$$

$$j_z Y_{j\Omega} = \Omega Y_{j\Omega}$$

$$j^2 Y_{j\Omega} = j(j + 1) Y_{j\Omega}$$

and

$$J^2 N_{M\Omega}^J = J(J + 1) N_{M\Omega}^J$$

$$J'_\pm N_{M\Omega}^J = \alpha_\mp(J, \Omega) N_{M\Omega \mp 1}^J$$

which come from the reversed commutation relations in the BF coordinates $[J_{x'}, J_{y'}] = -iJ_{z'}$ (Van Vleck 1951) we get

$$\langle j\Omega JM | l^2 | j\Omega \pm 1 JM \rangle = -\alpha_\pm(j, \Omega) \alpha_\pm(J, \Omega)$$

$$\langle j\Omega JM | l^2 | j\Omega JM \rangle = J(J + 1) + j(j + 1) - 2\Omega^2.$$

Then using equation (5) we get equation (9).

A3.2. V matrix elements

The matrix elements in the $|j\Omega JM\rangle$ basis may be expressed as

$$\langle j\Omega JM | V | j'\Omega' JM \rangle = \sum_{\lambda=0}^{\lambda_{\max}} \langle j\Omega | P_\lambda(\cos \Theta') | j'\Omega' \rangle v_\lambda(r)$$

where we have used equations (4), (10) and the normalization of the $N_{M\Omega}^J$. We have

$$\langle j\Omega | P_\lambda(\cos \Theta') | j'\Omega' \rangle = \delta_{\Omega\Omega'} (-)^{\Omega} [(2j + 1)(2j' + 1)]^{1/2} \begin{pmatrix} j & j' & \lambda \\ 0 & 0 & 0 \end{pmatrix} \begin{pmatrix} j & j' & \lambda \\ \Omega & -\Omega & 0 \end{pmatrix}.$$

Then using equation (5) we get equation (11).

References

- Abramowitz M and Stegun I A 1965 *Handbook of Mathematical Functions* (New York: Dover)
 Allison A C 1970 *J. Comput. Phys.* **6** 378–91
 Arthurs A M and Dalgarno A 1960 *Proc. R. Soc. A* **256** 540–51
 Choi B H and Tang K T 1975 *J. Chem. Phys.* **63** 1775–82
 Curtiss C F and Adler F T 1952 *J. Chem. Phys.* **20** 249–56
 De Vogelaere R 1955 *J. Res. Nat. Bur. Stand.* **54** 119–25
 Gordon R G 1971 *Meth. Comput. Phys.* **10** 81–109
 Gordon R G and Kim Y S 1972 *J. Chem. Phys.* **56** 3122–33
 Green S 1976 *Chem. Phys. Lett.* **38** 293–6
 Green S and Thaddeus P 1976 to be published

- Lester W A 1971 *Meth. Comput. Phys.* **10** 211–41
Light J C 1971 *Meth. Comput. Phys.* **10** 111–41
McGuire P 1976 *Chem. Phys.* **13** 81–94
McGuire P and Kouri D J 1974 *J. Chem. Phys.* **60** 2488–99
Neilsen W B and Gordon R G 1973 *J. Chem. Phys.* **58** 4131–48
Pack R T 1974 *J. Chem. Phys.* **60** 633–9
Rabitz H 1972 *J. Chem. Phys.* **57** 1718–25
Rose M E 1957 *Elementary Theory of Angular Momentum* (New York: Wiley)
Sams W N and Kouri D J 1969 *J. Chem. Phys.* **51** 4815–9
Van Vleck J H 1951 *Rev. Mod. Phys.* **23** 213–27
Walker R B and Light J C 1975 *Chem. Phys.* **7** 84–93